J Vet Sci. 2022 Nov;23(6):e70
https://doi.org/10.4142/jvs.22059
pISSN 1229-845X·eISSN 1976-555X

Journal of Veterinary Science

Original Article
Medical Imaging

Check for updates

CT imaging features of fat stranding in cats and dogs with abdominal disorder

Seolyn Jang [1], **Suhyun Lee** [1], **Jihye Choi** [2,*]

[1]Department of Veterinary Medical Imaging, College of Veterinary Medicine and BK 21 Plus Project Team, Chonnam National University, Gwangju 61186, Korea
[2]Department of Veterinary Medical Imaging, College of Veterinary Medicine, Seoul National University, Seoul 08826, Korea

OPEN ACCESS

Received: Mar 8, 2022
Revised: May 24, 2022
Accepted: Jun 21, 2022
Published online: Jul 26, 2022

***Corresponding author:**
Jihye Choi
Department of Veterinary Medical Imaging, College of Veterinary Medicine, Seoul National University, 1 Gwanak-ro, Gwanak-gu, Seoul 08826, Korea.
Email: imsono@snu.ac.kr
https://orcid.org/0000-0002-1258-7158

ABSTRACT

Background: Fat stranding is a non-specific finding of an increased fat attenuation on computed tomography (CT) images. Fat stranding is used for detecting the underlying lesion in humans.
Objectives: To assess the clinical significance of fat stranding on CT images for identifying the underlying cause in dogs and cats.
Methods: In this retrospective study, the incidence, location, extent, distribution, and pattern of fat stranding were assessed on CT studies obtained from 134 cases.
Results: Fat stranding was found in 38% (51/134) of all cases and in 35% (37/107) of tumors, which was significantly higher in malignant tumors (44%) than benign tumors (12%). Moreover, fat stranding was found in more than two areas in malignant tumors (16/33) and in a single area in benign tumors (4/4). In inflammation, fat stranding was demonstrated in 54% (7/13) in a single area (7/7) as a focal distribution (6/7). In trauma, fat stranding was revealed in 50% (7/14) and most were in multiple areas (6/7). Regardless of the etiologies, fat stranding was always around the underlying lesion and a reticular pattern was the most common presentation. Logistic regression analysis revealed that multiple areas ($p = 0.040$) of fat stranding and a reticulonodular pattern ($p = 0.022$) are the significant predictors of malignant tumor.
Conclusions: These findings indicated that CT fat stranding can be used as a clue for identifying the underlying lesion and can be useful for narrowing the differential list based on the extent and pattern.

Keywords: CT; mesentery; omentum; reticular; reticulonodular pattern

INTRODUCTION

The intraabdominal fat refers to the omentum, mesentery, pericolic fat, and the retroperitoneal fat [1]. The omentum and mesentery comprise a fatty tissue with abundant blood vessels and play an important role in the immune response, mediate the inflammatory response, repair the damaged tissue and provide wound isolation, and wrap the lesion providing a physical barrier to limit the spread of the abdominal infection [2]. Thus, various abdominal diseases including tumors, inflammation, and trauma can induce changes in

ORCID iDs
Seolyn Jang
https://orcid.org/0000-0001-5757-6893
Suhyun Lee
https://orcid.org/0000-0002-3153-0691
Jihye Choi
https://orcid.org/0000-0002-1258-7158

Author Contributions
Conceptualization: Choi J; Data curation: Jang S, Lee S; Formal analysis: Jang S, Choi J; Funding acquisition: Choi J; Investigation Jang S, Choi J; Methodology: Jang S; Project administration: Choi J; Software: Jang S, Lee S; Supervision: Choi J; Validation: Jang S, Choi J; Writing - original draft: Jang S; Writing - review & editing: Jang S, Lee S, Choi J.

Conflict of Interest
The authors declare no conflicts of interest.

Funding
This research was supported by the Animal Medical Institute of Seoul National University and Basic Science Research Program through the National Research Foundation of Korea (NRF), funded by the Ministry of Science, ICT, and Future Planning (NRF-2018R1A2B6006775).

the fat due to edema or a defect in the lymphatic drainage [3]. The omentum consists of the greater omentum and lesser omentum. The greater omentum covers the abdominal structures and attaches to the greater curvature of the stomach to the urinary bladder and ventral surface of the transverse colon bilaterally [4-6]. The lesser omentum connects the lesser curvature of the stomach to the liver and cranial part of the duodenum [5]. The mesentery is a contiguous structure which arises from the mesenteric root and spreads to the intestine radially from the duodenum to the rectum [7].

On computed tomography (CT), fat appears as a homogeneous hypoattenuation (–100 to –160 Hounsfield unit [HU]) [8,9]. However, fat attenuation can be increased to –40 to –60 HU in several pathologic conditions including inflammation, ischemia, tumor, trauma, and irritation caused by peritoneal effusion or surgical manipulation [10-19]. A non-specific finding of an increased attenuation in fat on CT images is referred to as fat stranding. Fat stranding can be visualized in various appearances on CT images depending on the cause and chronicity of the underlying lesion; a ground glass pattern is usually visualized in mild inflammation [20]. Furthermore, a reticular pattern indicates severe inflammation. A reticulonodular pattern is mainly observed with fat infiltration of the tumor or carcinomatosis [20].

Fat stranding is used for detecting the underlying lesion in humans. For example, the edematous change of the pericholecystic fat can indicate acute cholecystitis, accompanied by wall thickening, gall bladder distention, pericholecystic fluid, and high-attenuation bile [11]. When the attenuation of fat stranding is higher than that of the underlying bowel wall thickness, disproportionate fat stranding helps in diagnosing diseases originating from the mesentery or omentum, such as diverticulitis, acute appendicitis, epiploic appendicitis, and omental infarction in patients with acute abdomen [13]. However, based on our review of the literature, there have been no reports about CT fat stranding in veterinary medicine.

Therefore, in this study, we assessed the correlation between the presence and characteristics of fat stranding on CT studies and its etiology. The purpose of this study was to assess the clinical significance of fat stranding for identifying the underlying lesion and narrowing the differential list. We hypothesized that comprehensive assessment in patterns and location of fat stranding could help in detecting the underlying lesion accurately and discriminating malignant tumors from benign tumors.

MATERIALS AND METHODS

The study protocol was approved by the Institutional Animal Care and Use Committee at Chonnam National University (CNU IACUC-YB-2021-54).

Animal selection

This retrospective study reviewed the CT studies of dogs and cats conducted at Chonnam National University Veterinary Teaching Hospital from January 2014 to April 2020. The inclusion criteria were as follows: 1) the quality of the CT studies was sufficiently good for interpreting the fat, 2) no evidence of hypoalbuminemia and right heart failure which induced the general edema, and 3) no evidence of large amount of abdominal fluid which obscured abdominal organs and fat. The decision regarding the inclusion of dogs and cats in the study was made by two veterinarians (S.L.J. and S.H.L.) with 2 years of radiology

experience. The medical records were reviewed for the signalment (age, breed, sex, and weight) and chief complaint, and the indication for the CT examination was classified into tumor (benign vs. malignant), inflammatory disease, and trauma.

CT study

CT scans were conducted under general anesthesia in all animals. The induction of anesthesia was performed by the intravenous injection of a combination of 0.2 mg/kg butorphanol (Butophan; Myungmoon Pharm, Korea), 0.2 mg/kg midazolam (Midacum; Myungmoon Pharm), and 4 mg/kg propofol (Probive; Myungmoon Pharm), and the anesthesia was maintained with isoflurane (Terrell 1%–2%; Piramal Critical Care, USA) and oxygen (1 L/min). The animals were positioned in a sternal recumbency, and pre- and post-contrast CT studies were obtained using a 16-channel multidetector CT scanner (Siemens Emotion 16; Siemens, Germany) with the following settings: slice thickness = 1–2 mm; pitch = 0.8–1.5; rotation duration = 600 ms; tube voltage = 120–130 kV; and tube current = 110–130 mA. Contrast study was performed after the injection of 600 mgI/kg of Iohexol (Omnipaque 300; GE Healthcare, Norway) at a rate of 1.5–3.0 mL/sec using a power injector (MEDRAD Vistron CT injection system; MedRad, USA) or via manual injection through 24- to 22-gauge intravenous catheters. The breath-hold technique was employed to minimize respiration-related motion artifacts prior to CT scan. Then, CT images were reconstructed into sagittal and dorsal planes with a setting of 0.7–1.5 mm thickness and 0.8–1 mm interval.

Image analysis

All CT studies were evaluated at workstation using PACS (Infinitt PACS; Infinitt Healthcare, Korea) individually by two veterinarians (J.S.L and L.S.H.) with 2 years of radiology experience), under the supervision of one professor of veterinary radiology (J.H.C) with a 23-year experience of radiology. The CT assessment was performed in a blinded manner to the indication of CT study and other reader's data. However, it could not be completely blind for the veterinarians who selected the cases. CT images were assessed with a window width of 400 HU and a window level of 40 HU, and further adjustment of the window settings was allowed as each reader's desire.

Fat stranding was assessed as to the location, extent, distribution, and pattern on CT images (**Fig. 1**). The location of fat stranding was classified into four areas: omentum, mesentery, retroperitoneum, and pericolic area [1]. The extent was classified depending on the number of the involved area of fat stranding: single if fat stranding is defined to one area, multiple if more than two or three areas excluding the retroperitoneum and generalized if fat stranding spans more than three areas including the retroperitoneum. The distribution of fat stranding was assessed in each area and subdivided into focal, multifocal, and diffuse. The pattern of fat stranding was classified as ground-glass, reticular, and reticulonodular patterns: a subtle hazy increase of fat attenuation as a ground-glass pattern, a well-defined linear area of increased attenuation as a reticular pattern, and combined linear and nodular areas of increased attenuation as a reticulonodular pattern [20]. When more than two patterns were observed, the fat stranding was classified according to the more obvious and severe pattern, determined in order of severity as follows: ground glass, reticular, and reticulonodular patterns.

Statistical analysis

The statistical analysis was performed by one veterinarian (S.L.J), under the supervision of one statistician (J.K.K) using SPSS version 23.0 (IBM SPSS Statistics for Windows; IBM Corp., USA). The difference in the pattern, location, extent, and distribution of fat stranding

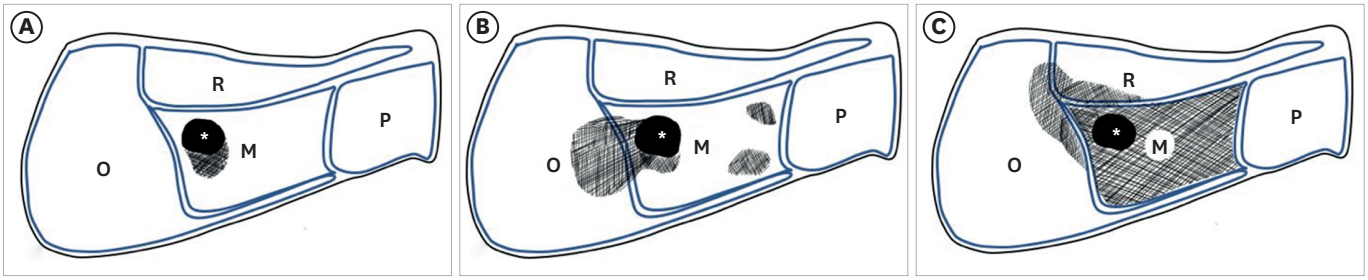

Fig. 1. Schematic diagram of the location, extent, and distribution of fat stranding. The abdominal cavity is divided into the omentum, mesentery, retroperitoneum, and pericolic areas. (A) Fat stranding (dark area) adjacent to the mass (asterisk) is found in the mesentery and classified as a single extent with focal distribution. (B) Fat stranding is observed in both the omentum and mesentery and classified as multiple extent. In the mesentery, multifocal fat stranding is distributed separately within the area. (C) Fat stranding is identified in three areas including the retroperitoneum and classified as a generalized extent. In the mesentery, since fat stranding is distributed in most areas, it is classified as diffuse distribution and the omentum and retroperitoneum as focal distribution. O, omentum; M, mesentery; R, retroperitoneum; P, pericolic.

in the CT images between malignant and nonmalignant lesions including benign tumor, inflammation, and trauma was assessed using a univariate multiple logistic regression analysis. The level of significance was set at $p < 0.05$. The positive predictive value for the diagnosis of malignant tumor by fat stranding pattern and extent was calculated using the histologic diagnosis as the gold standard. The interobserver agreement in the assessment of the pattern, location, extent, and distribution of fat stranding was assessed using Cohen's kappa coefficient (κ). Inter-observer correlation was evaluated as < 0.4, poor agreement; 0.41–0.6, moderate agreement; 0.61–0.8, good agreement; and > 0.8, excellent agreement. The mean value of the two readers' results was used for data analysis.

RESULTS

In this study, the abdominal CT studies were reviewed in 134 patients including 107 tumors, 13 inflammatory diseases, and 14 trauma cases. Among them, 51 patients showed fat stranding in CT studies, including 45 dogs and 6 cats (**Table 1**). The etiology for fat stranding was classified as tumor (n = 37), inflammation (n = 7), and trauma (n = 7) according to laboratory test, cytology, and histopathologic examinations (**Table 2**). The underlying abdominal lesions of fat stranding were observed on CT study in 46 patients; as single lesion in 41 cases or multiple lesions in 5 cases. In the remaining 5 animals, fat stranding was found without an abdominal lesion on CT study that was performed due to trauma (n = 4) or panniculitis (n = 1).

The locations of the abdominal lesions and fat stranding are presented in **Table 3**. All fat stranding was found adjacent to the abdominal lesions regardless of the etiology. Most of

Table 1. Signalments of 51 animals with fat stranding on CT images

Signalments	Animal (n = 51)
Sex	14 intact female, 15 female spayed, 5 intact male, and 17 castrated male
Age (yr)	Median 10 years (range; 1–16 years)
Species and breed (number)	Dog (45) Shih-tzu (n = 9), Maltese (n = 8), Schnauzer (n = 6), Poodle (n = 4), Golden Retriever (n = 3), French Bulldog (n = 2), Mongrel (n = 2), Miniature Pinscher (n = 2), Bull Terrier (n = 1), Cocker spaniel (n = 1), Jack Russel Terrier (n = 1), Jindo (n = 1), Pekingese (n = 1), Shar Pei (n = 1), Shiba Inu (n = 1), Yorkshire Terrier (n = 1), and West Highland White Terrier (n = 1). Cats (6) Korean Short Hair (n = 4), Persian (n = 1), and Turkish Angora (n = 1)

CT, computed tomography.

Table 2. Causes and underlying lesions of fat stranding identified in 46 animals

Tumor (n = 37)		Inflammation (n = 7)	Trauma (n = 7)
Malignant (n = 33)	Benign (n = 4)		
Adenocarcinoma (5): small intestine (3), large intestine, kidney and urinary bladder metastasis	**Lipoma (1):** omentum	**Pancreatitis (3):** pancreas	**Falling injury (1):** abdominal wall
Hepatocellular carcinoma (5): liver (4), liver and kidney	**Adenoma (1):** kidney	**Pyonephritis (1):** kidney	**Biting wound (1):** abdominal wall
Hemangiosarcoma (4): spleen (3), multicenteric[b]	**Parovarian cyst (1):** ovary	**Feline infectious peritonitis (1):** large intestine	**Hit by car (1):** abdominal wall
High grade sarcoma (1): spleen	**Hematoma (1):** spleen	**Granulomaous myositis (1):** sublumbar muscle	**Traffic accident (4)**[a]
Lymphoma (4): kidney, spleen (2), liver and sublumbar lymph node		**Panniculitis (1)**[a]	
Fibrosarcoma (2): spleen, small intestine metastasis			
Gastric carcinoma (1): stomach			
Extraskeletal osteosarcoma (1): small intestine			
Transitional cell carcinoma (1): urinary bladder			
Soft tissue sarcoma (1): abdominal wall metastasis			
Malignant suspected (5): sublumbar muscle, spleen), kidney, small intestine, liver and sublumbar muscle			
Melanoma metastasis (1): kidney			
Sclerosing carcinoma (1): retroperitoneal mass			
Ovarian carcinoma (1): ovary			

[a]No abdominal lesion; [b]Many abdominal lesions are scattered throughout the abdominal cavity to counting the number of lesion. So excluded from counting the number of lesion.

Table 3. Location of the underlying abdominal lesion and fat stranding on CT images

Etiology	Mesentery	Omentum	Retroperitoneum	Pericolic
Underlying lesions (n = 49)				
Tumor	9	19	10	2
Malignant	8	17	9	2
Benign	1	2	1	0
Inflammation	0	3	2	1
Trauma	1	1	0	1
Total	10	23	12	4
Fat stranding (n = 78)				
Tumor	14	24	12	8
Malignant	13	22	11	8
Benign	1	2	1	0
Inflammation	0	3	3	1
Trauma	1	1	6	5
Total	15	28	21	14

CT, computed tomography.

the abdominal lesion and fat stranding were located in the omentum or retroperitoneum. Abdominal lesions were only found in the pericolic area in three dogs; however, fat stranding in the pericolic area (18%) and the mesentery (19%) was frequently found.

The extent of fat stranding in the 51 cases was determined as single (n = 27), multiple (n = 22), or generalized (n = 2). In tumors (n = 37), the number of fat stranding was found as single in 19 and multiple in 32. In benign tumors, all fat stranding was found in a single area (n = 4); however, malignant tumors generated fat stranding in 15 single areas and 32 multiple areas. All inflammatory diseases were accompanied by fat stranding in single areas, while trauma always showed fat stranding in multiple areas except for one case.

The distribution of fat stranding in each area is presented in **Table 4**. Multiple fat stranding was found in malignant tumors and trauma. Generalized fat stranding spanning more than three areas was detected in two dogs with malignant tumors.

Table 4. Distribution of fat stranding in each area according to the etiology

Etiology	Single (n = 27)			Multiple (n = 44)		
	Focal	Multifocal	Diffuse	Focal	Multifocal	Diffuse
Tumor	7	9	3	12	4	16
Malignant	5	8	2	12	4	16
Benign	2	1	1	0	0	0
Inflammation	6	0	1	0	0	0
Trauma	1	0	0	2	2	8

A single mass was found in all benign tumors (n = 4). Moreover, fat stranding in benign tumors was also found in a single area around the tumor, which presented with focal, multifocal, or diffuse distribution.

Most malignant tumors were located at a single area (n = 28). Meanwhile, about 50% of fat stranding in malignant tumors were found in more than two areas with multifocal distribution. Most multiple fat stranding was concurrently found in the mesentery and omentum (n = 7) which were associated with adenocarcinoma of the small intestine (n = 3), splenic hemangiosarcoma (n = 1), hepatocellular carcinoma (n = 1), soft tissue sarcoma of the left abdominal wall (n = 1), and fibrosarcoma of the small intestine (n = 1). In one dog with splenic hemangiosarcoma and one dog with small intestine adenocarcinoma, fat stranding was found in the omentum and pericolic area, respectively. Concurrence of fat stranding in the retroperitoneum and intra-abdominal areas was shown in seven animals: at the pericolic area in retroperitoneal tumors (n = 3) and transitional cell carcinoma of the urinary bladder (n = 1); mesentery in multicentric lymphoma (n = 1); omentum in multicentric lymphoma (n = 1) and hepatocellular carcinoma (n = 1). In a dog with multicentric hemangiosarcoma, generalized fat stranding features showed multiple nodules in the subcutaneous fat and peritoneal and retroperitoneal spaces, lungs, pleural wall, and myocardium (**Fig. 2**). The other dog with generalized fat stranding had a retroperitoneal tumor from the 5th lumbar area to the rectum and metastasis to the liver and spleen. The fat stranding was found in the retroperitoneum, omentum around the liver and spleen, and in the pericolic area.

Fat stranding in inflammatory diseases (n = 7) was found in three dogs with pancreatitis, pyonephritis of the left kidney, pyogranulomatous panniculitis, and granulomatous myositis in the sublumbar region in each dog and feline infectious peritonitis in one cat.

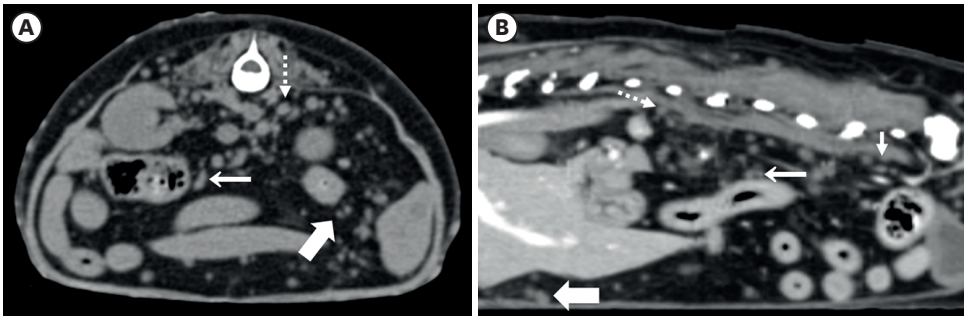

Fig. 2. Generalized fat stranding in an 11-year-old, neutered male dog with multicentric hemangiosarcoma. Pre contrast transverse (A) and contrast enhanced sagittal (B) planes of the CT study show multiple nodules and fat stranding in the subcutaneous, mesentery, (thin arrow), omentum (thick arrow), retroperitoneum (dotted arrow), and pericolic area (short arrow). CT images are presented on the soft tissue window (window width = 400 HU, window level = 40 HU).
CT, computed tomography; HU, Hounsfield unit.

https://doi.org/10.4142/jvs.22059

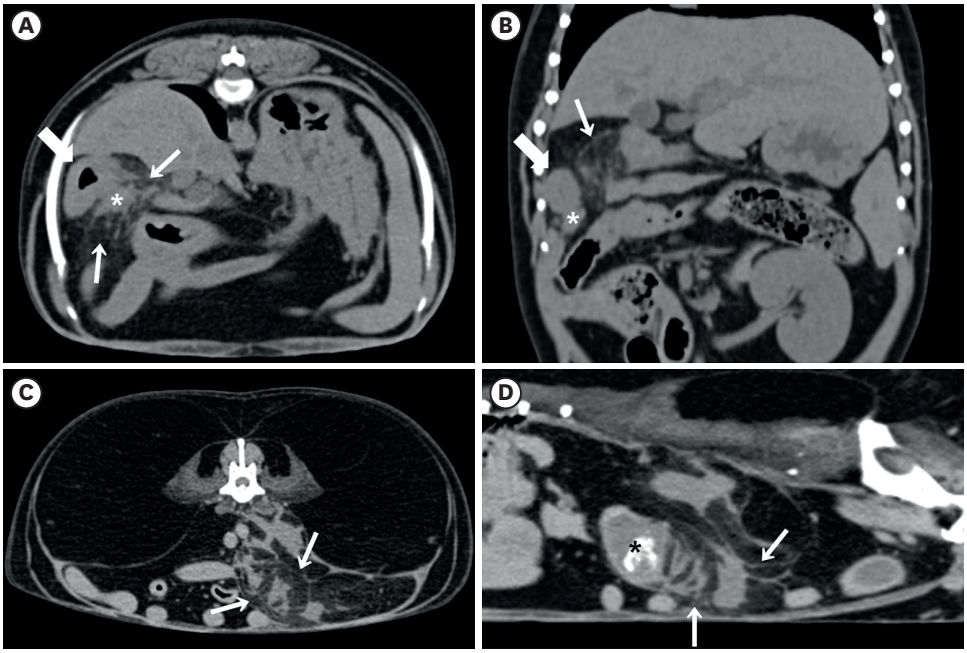

Fig. 3. CT images of fat stranding in a 12-year-old, spayed female dog with acute pancreatitis (A, B) and a 13-year-old, spayed female dog with severe pyonephritis (C, D). (A) In acute pancreatitis with extrahepatic bile duct obstruction, the peripancreatic fat (thin arrows) is marked swollen around the duodenum (thick arrow) and the right lobe of the pancreas (asterisk) in the right upper quadrant. Fat stranding is found in a single area, the omentum, as a focal lesion on the transverse plane. On transverse (C) and sagittal (D) planes of the CT study in a dog with severe pyonephritis of the left kidney, diffuse linear fat stranding (arrows) with free fluid is found in the ipsilateral retroperitoneum and pericolic region. Most of the parenchyma of the left kidney is lost and the renal pelvis is dilated with multiple stones (asterisk). CT images are presented on the soft tissue window (window width = 400 HU, window level = 40 HU).
CT, computed tomography; HU, Hounsfield unit.

All inflammatory lesions were found in a single area. Fat stranding was also found in a single area (n = 7) as a focal distribution (n = 6) around the abdominal lesion. For example, in one dog, severe pancreatitis with concurrent extrahepatic bile duct obstruction induced fat stranding broadly; however, it was located within the omentum around the pancreas as a focal lesion (**Fig. 3A and B**). Meanwhile, in one dog with severe pyonephritis, diffuse distribution of fat stranding was found from the perirenal region to the ipsilateral retroperitoneum; however, fat stranding was found only in the retroperitoneal space as a single lesion (**Fig. 3C and D**).

Of the 14 patients with trauma, fat stranding was observed in 5 dogs and 2 cats (50%). The trauma occurred by traffic accident with an accompanying hind limb fracture in five patients, bite wounds with a comminuted lumbar fracture in one dog, and falling resulting in spinal cord compression in one cat. Among the 7 patients with trauma as a cause of fat stranding, 6 had it in multiple areas. A CT examination was conducted 2–5 days after the accident. Conversely, in one cat with fat stranding in a single area, CT examination was performed due to problems with defecation secondary to a megacolon caused by a pelvic fracture 4 years prior. In trauma with multiple area involvement, focal distribution of fat stranding was found in a bite wound (n = 1), and diffuse edematous change in the pericolic and caudal retroperitoneum was observed in traffic accidents (n = 4).

The reticular pattern was the most common CT appearance of fat stranding in all animals regardless of the etiology (38/51) (**Table 5**). Meanwhile, about 33% of malignant tumors

(11/33) had the reticulonodular pattern, particularly in adenocarcinoma with carcinomatosis, lymphosarcoma, splenic hemangiosarcoma, gastric carcinoma, metastatic fibrosarcoma with sarcomatosis, and multicentric subcutaneous hemangiosarcoma (**Fig. 4**). One dog with pyogranulomatous panniculitis also showed the reticulonodular pattern (**Fig. 5**). Ground-glass pattern was observed in almost all animals with other types of fat stranding and only one dog with benign infiltrative lipoma showed fat stranding with ground-glass pattern in the omentum without other patterns.

Table 5. Fat stranding patterns according to the etiology

Pattern	Tumor (n = 37)		Inflammation (n = 7)	Trauma (n = 7)
	Malignant (n = 33)	Benign (n = 4)		
Ground-glass	0	1	0	0
Reticular	22	3	6	7
Reticulonodular	11	0	1	0

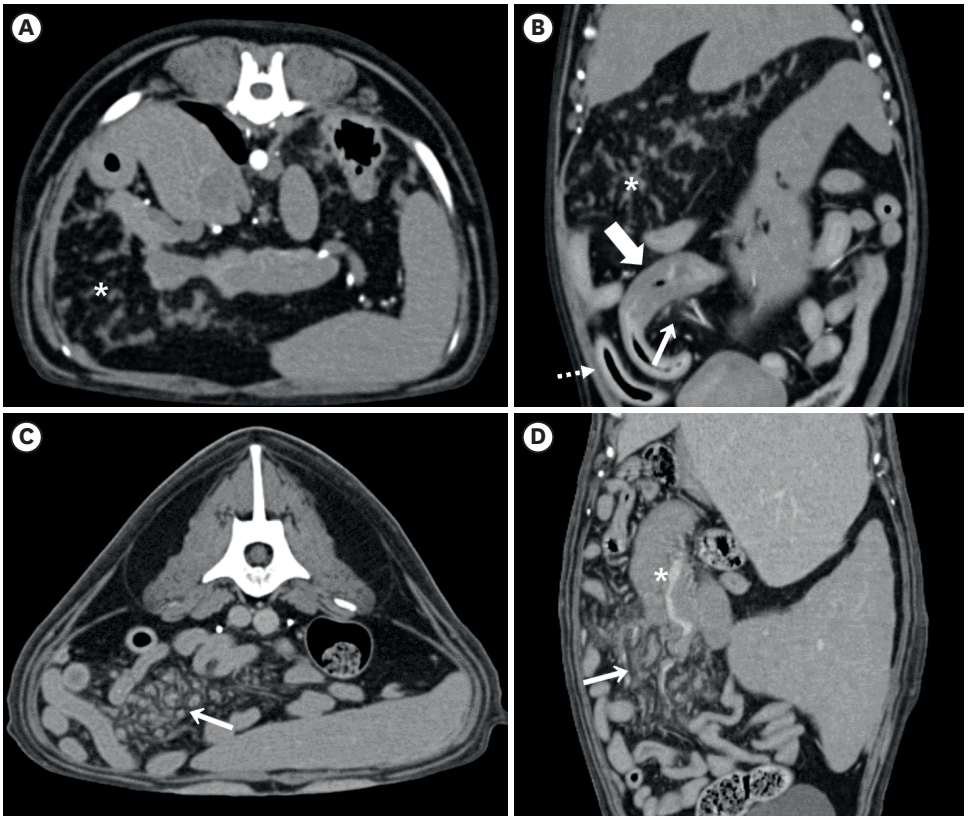

Fig. 4. Fat stranding with a reticulonodular pattern in malignant tumors. On transverse (A) and dorsal (B) planes of the CT study in a 10-year-old, neutered male dog with adenocarcinoma originating from the colon, the colon (thick arrow) is thickened circumferentially with 8-mm thickness and shows low enhancement compared to the adjacent intestinal wall (dotted arrow). The reticular pattern fat stranding (thin arrow) is observed with the jejunal artery caudal to the colonic mass. In addition, amorphous linear fat stranding and multiple nodularity are found throughout the omentum (asterisk) from the caudal margin of the liver to the mesenteric root. Transverse (C) and dorsal (D) planes of CT study in a 7-year-old, intact female dog with left scapular fibrosarcoma with mesenteric sarcomatosis. The ileocolic lymph nodes (asterisk) are enlarged with an irregular caudal margin. At the right middle abdominal quadrant, many nodules are present in the thickened mesentery (arrow). CT images are presented on the soft tissue window (window width = 400 HU, window level = 40 HU).
CT, computed tomography; HU, Hounsfield unit.

https://doi.org/10.4142/jvs.22059

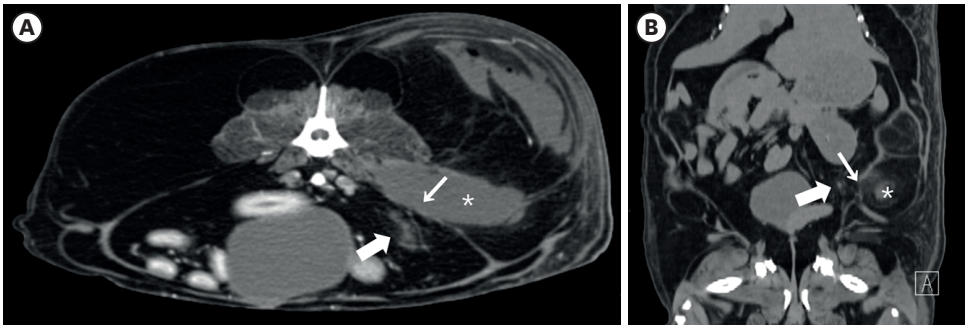

Fig. 5. Transverse (A) and dorsal (B) planes of the CT image of an 11-year-old, intact female dog with pyogranulomatous subcutaneous panniculitis with retroperitoneal space infiltration. The defect of the left abdominal wall at the level of the retroperitoneal space between the retroperitoneum and subcutaneous was not observed clearly (thin arrow), and fat stranding with reticulonodular pattern is focally observed in the caudal part of retroperitoneum (thick arrow). Extensive subcutaneous fat hyper-attenuation with striations is observed (asterisk). CT images are presented on the soft tissue window (window width = 400 HU, window level = 40 HU). CT, computed tomography; HU, Hounsfield unit.

The difference in the CT appearance in pattern, location, extent, and distribution of fat stranding between malignant and nonmalignant causes including benign tumor, inflammation, and trauma was assessed. Multiple areas in the extent of fat stranding showed that the probability of being malignant was 2.67 times higher than that of the non-malignant tumor group (95% confidence interval [CI], 0.147–0.958; $p = 0.040$) when compared to a single area. The reticulonodular pattern showed that the probability of malignancy was about 11 times higher than the reticular pattern (95% CI, 1.420–85.201; $p = 0.022$). The positive predictive value of the multiple extent and reticulonodular pattern on CT was 73% and 92% for the malignant tumor, respectively. Interobserver agreement of the CT assessments is presented in **Table 5**. The assessment for the extent ($\kappa = 0.828$) and location ($\kappa = 0.801$) of fat stranding had excellent agreement. Fat stranding pattern and distribution within the area showed a good agreement ($\kappa = 0.783$).

DISCUSSION

This study evaluated fat stranding on CT images regarding the incidence, location, extent, distribution, and pattern in dogs and cats. The location, extent, and pattern of fat stranding were helpful for the localization of the underlying lesion or predicting malignancy.

Fat stranding was found around the abdominal lesion in all animals regardless of the etiology. Similarly, in humans, fat stranding is used to identify the pathologic lesion because it is usually found adjacent to the underlying lesions [20]. The close anatomic relation between fat stranding and the underlying lesion can be explained through the pathogenesis of fat stranding [7,20]. For instance, in inflammation such as pancreatitis, the disturbance of parenchymal microcirculation and stimulation of apoptosis lead to parenchymal edema and peripancreatic inflammation which result in hazy or reticular stranding of the peripancreatic fat [15,16]. In tumors, fat stranding develops by the direct invasion of the primary tumor into the adjacent peritoneal ligament, through tumor secretion and metastatic cell growth within the compartment near the tumor or by the metastatic nodules which usually develop near the primary tumor in carcinomatosis [3,12,21,22]. In trauma, bleeding and cellular infiltration are manifested as fat stranding and found along the vessels near the traumatic

https://doi.org/10.4142/jvs.22059

region via a shearing force, increased intraluminal pressure, or direct injury [23,24]. These mechanisms associated with the etiology finally induce edema or lymphatic drainage failure that causes fat stranding near the site of the pathology [7,20]. In our study, fat stranding was even demonstrated without any abdominal lesion in four dogs, which encountered traffic accidents, as diffuse edematous change adjacent to the region affected by the trauma. Similarly, in some human blunt trauma patients, the damaged organ was not detected at an early stage after trauma, while an increased fat density by diffuse or focal infiltration of the microhemorrhage was identified in advance and was clinically useful for identifying the damaged organ [23,24]. In one dog with subcutaneous panniculitis, fat stranding in the retroperitoneum allowed the detection of the spread of inflammation into the retroperitoneum, although the abdominal muscle defect between the subcutaneous region and retroperitoneum was not clearly observed on CT images.

The extent of the fat stranding was related with the etiology in this study. In benign tumors and inflammatory diseases, both the abdominal lesion and fat stranding were found in the same single area. Within the area, fat stranding showed focal distribution around the abdominal lesion. Even when the attenuation of the retroperitoneal fat was diffusely increased in a dog with severe pyonephritis, the fat stranding did not spread to other areas in the abdomen. This may be due to the peritoneal defense mechanisms for wound isolation which prevents the spread of the abdominal infection by wrapping around the lesion. In addition, the omentum and mesentery act as boundaries for pathological processes for disease localization [22,25-27]. In patients of severe inflammatory disease such as necrotic pancreatitis, local inflammation can spread over the surrounding tissue or even progress to a systemic response and cause fat stranding in remote places apart from the lesion [4,5,28]. However, because our study focused on assessing fat stranding in inflammatory diseases, focal inflammatory diseases such as mild pancreatitis or pyonephritis were mainly included. Whereas, when severe or generalized inflammatory diseases caused ascites or obscured fat stranding, they were excluded from our study.

In this study, fat stranding was found in multiple areas with diffuse distribution in several malignant tumors. Tumor can spread to the peritoneal cavity in four major ways via a direct invasion, lymphatic extension, embolic hematogenous spread, or intraperitoneal seeding [22]. Among them, direct invasion and lymphatic extension occur commonly through peritoneal ligaments that interconnect the abdominal viscera. In our study, the concurrent involvement of the mesentery and omentum was the most common. In addition, fat stranding covering the retroperitoneum with mesentery or omentum was found in three dogs with multicentric lymphoma and hepatocellular carcinoma. This result may be related to the anatomic connection between the peritoneal cavity and retroperitoneum via the abdominal ligaments [29]. That is, a pair of gastrohepatic and hepatoduodenal ligament, a pair of gastrosplenic and splenorenal ligament, and a pair of the gastrocolic and transverse mesocolon interconnect the abdominal organs together and establish bridges to the retroperitoneum [22]. Thus, diseases of the abdominal organs can spread to the retroperitoneum via this connection. However, since the peritoneal and retroperitoneal cavities are separated by the peritoneum, which acts as a barrier, the spread of malignant tumor between the two cavities is less common compared to the spread within the peritoneal cavity. In animals with retroperitoneal fat stranding, fat stranding in the pericolic area are more common than in the mesentery or omentum since the pericolic fat is defined as fat surrounding the colon and stratified into the subserosal, retroperitoneal, and the mesenteric fat [14,30].

https://doi.org/10.4142/jvs.22059

In humans, the CT pattern approach is used for classifying fat stranding such as smooth regular, irregular, and nodular patterns or ground-glass, reticular, and reticulonodular patterns [20,21]. This CT pattern approach is a useful diagnostic tool for differentiating benign peritoneal disease from malignancy because the prevalent pattern is determined according to the malignant potential of the underlying lesion [21]. The CT appearance of fat stranding in the omentum and mesentery is dependent on the duration of the disease [26]. It presents as a smudged appearance in the early stage, and as the disease progresses, soft tissue nodules form. In our study, the reticular pattern was most common one, regardless of the etiology of fat stranding. In the univariate logistic regression analysis of malignancy by fat stranding pattern, the reticulonodular pattern was statistically significant with an odds ratio of 11.0. That is, the reticulonodular pattern in our study was associated with a malignant tumor, similar to human studies [20,21]. However, this result did not mean that the reticulonodular pattern was a pathognomonic feature for a malignant tumor, because this pattern was also observed in severe inflammation such as severe pyogranulomatous panniculitis in a dog. Similarly, in humans, fat stranding with a reticulonodular pattern is also reported in inflammatory diseases by fatty inflammation and fibrosis such as mesenteric panniculitis or tuberculosis although less common compared to malignant tumors [26,31]. In humans, a ground-glass pattern is most often caused by mild inflammation and the reticular pattern is found with increasing severity of the inflammation [20]. In our study, the ground-glass pattern was found in almost all CT studies accompanied with reticular or reticulonodular patterns. In our study, fat stranding pattern was classified as the more severe form, such as reticular or reticulonodular pattern, when there were more than two patterns of fat stranding. Following the CT pattern approach for classifying fat stranding [20,21], only one dog with omental lipoma was classified as having a ground-glass pattern. However, the propensity of the ground-glass and reticular patterns to distinguish between malignant tumors and benign disease is limited. Since either malignant or benign disease can result in the infiltration of peritoneal fat and the CT appearance varies greatly, interpretation of fat stranding with other CT findings in the adjacent structures, such as mesenteric root involvement, edematous change of subcutaneous fat, preservation of other fatty area, and adjacent organ edema, will allow accurate differentiation between inflammation or neoplastic disease [32,33].

This study has some limitations. First, the total population of this study has a small sample size and only a small number of dogs with benign tumors was included in tumor group compared to the malignant tumor group. Second, the effect of the small amount of abdominal fluid that was not caused by hypoalbuminemia or liver pathology was not considered in the evaluation of fat stranding.

This study indicated that fat stranding is relatively common in the CT studies of dogs and cats with tumors, inflammation, or trauma. Fat stranding can be used as an important clue in identifying the abdominal lesion and can be useful for narrowing the differential diagnosis based on the extent and pattern of fat stranding. A malignant etiology can be suspected if a reticulonodular pattern of fat stranding is found in multiple areas. In addition, if fat stranding is found in a single area and is a focally distributed, inflammation or benign tumor can be considered.

REFERENCES

1. Djmel E, Jrad M, Ben Temellist L, Zrelly R, Mizouni H. The peritoneum: anatomy & pathological processes. In: Proceedings of European Congress of Radiology-ECR 2017; 2017 Mar 1-5; Vienna. Vienna: European Society of Radiology; 2017, C-1395.
CROSSREF
2. Meza-Perez S, Randall TD. Immunological functions of the omemtum. Trends Immunol. 2017;38(7):526-536.
PUBMED | CROSSREF
3. Mindelzun RE, Jeffrey RB Jr, Lane MJ, Silverman PM. The misty mesentery on CT: differential diagnosis. AJR Am J Roentgenol. 1996;167(1):61-65.
PUBMED | CROSSREF
4. Healy JC, Reznek RH. The peritoneum, mesenteries and omenta: normal anatomy and pathological processes. Eur Radiol. 1998;8(6):886-900.
PUBMED | CROSSREF
5. Doom M, de Rooster H, van Bergen T, Gielen I, Kromhout K, Simoens P, et al. Morphology of the canine omentum part 2: the omental bursa and its compartments materialized and explored by a novel technique. Anat Histol Embryol. 2016;45(1):28-36.
PUBMED | CROSSREF
6. Doom M, de Rooster H, van Bergen T, Gielen I, Kromhout K, Simoens P, et al. Morphology of the canine omentum part 1: arterial landmarks that define the omentum. Anat Histol Embryol. 2016;45(1):37-43.
PUBMED | CROSSREF
7. Coffey JC, O'Leary DP. The mesentery: structure, function, and role in disease. Lancet Gastroenterol Hepatol. 2016;1(3):238-247.
PUBMED | CROSSREF
8. Mauad FM, Chagas-Neto FA, Benedeti AC, Nogueira-Barbosa MH, Muglia VF, Carneiro AA, et al. Reproducibility of abdominal fat assessment by ultrasound and computed tomography. Radiol Bras. 2017;50(3):141-147.
PUBMED | CROSSREF
9. Chang J, Jung J, Lee H, Chang D, Yoon J, Choi M. Computed tomographic evaluation of abdominal fat in minipigs. J Vet Sci. 2011;12(1):91-94.
PUBMED | CROSSREF
10. Seo IK, Kim BJ, Kim B, Choi CH, Kim JW, Kim JG, et al. Abdominal fat distribution measured using computed tomography is associated with an increased risk of colorectal adenoma in men. Medicine (Baltimore). 2017;96(37):e8051.
PUBMED | CROSSREF
11. Fidler J, Paulson EK, Layfield L. CT evaluation of acute cholecystitis: findings and usefulness in diagnosis. AJR Am J Roentgenol. 1996;166(5):1085-1088.
PUBMED | CROSSREF
12. Patel CM, Sahdev A, Reznek RH. CT, MRI and PET imaging in peritoneal malignancy. Cancer Imaging. 2011;11(1):123-139.
PUBMED | CROSSREF
13. Pereira JM, Sirlin CB, Pinto PS, Jeffrey RB, Stella DL, Casola G. Disproportionate fat stranding: a helpful CT sign in patients with acute abdominal pain. Radiographics. 2004;24(3):703-715.
PUBMED | CROSSREF
14. Morimoto T, Yamada T, Miyakawa K, Nakajima Y. Factors associated with pericolic fat stranding of colon cancer on computed tomography colonography. Acta Radiol Open. 2018;7(2):2058460118757578.
PUBMED | CROSSREF
15. Türkvatan A, Erden A, Türkoğlu MA, Seçil M, Yener Ö. Imaging of acute pancreatitis and its complications. Part 1: acute pancreatitis. Diagn Interv Imaging. 2015;96(2):151-160.
PUBMED | CROSSREF
16. O'Connor OJ, Buckley JM, Maher MM. Imaging of the complications of acute pancreatitis. AJR Am J Roentgenol. 2011;197(3):W375-81.
PUBMED | CROSSREF
17. Garland J, Olds K, Tse R. Perinephric fat stranding on postmortem computed tomography scan in acute pyelonephritis: a case report. Am J Forensic Med Pathol. 2019;40(4):391-393.
PUBMED | CROSSREF
18. Oei TN, Jagannathan JP, Ramaiya N, Ros PR. Peritoneal sarcomatosis versus peritoneal carcinomatosis: imaging findings at MDCT. AJR Am J Roentgenol. 2010;195(3):W229-35.
PUBMED | CROSSREF

19. Sartelli M, Moore FA, Ansaloni L, Di Saverio S, Coccolini F, Griffiths EA, et al. A proposal for a CT driven classification of left colon acute diverticulitis. World J Emerg Surg. 2015;10:3.
PUBMED | CROSSREF
20. Thornton E, Mendiratta-Lala M, Siewert B, Eisenberg RL. Patterns of fat stranding. AJR Am J Roentgenol. 2011;197(1):W1-14.
PUBMED | CROSSREF
21. Filippone A, Cianci R, Delli Pizzi A, Esposito G, Pulsone P, Tavoletta A, et al. CT findings in acute peritonitis: a pattern-based approach. Diagn Interv Radiol. 2015;21(6):435-440.
PUBMED | CROSSREF
22. Brink JA, Wagner BJ. Pathways for the spread of disease in the abdomen and pelvis. In: Hodler J, Kubik-Huch RA, von Schulthess GK, editors. *Diseases of the Abdomen and Pelvis 2018-2021: Diagnostic Imaging*. Wallisellen: IDKD Book; 2018, 57-65.
23. Iaselli F, Mazzei MA, Firetto C, D'Elia D, Squitieri NC, Biondetti PR, et al. Bowel and mesenteric injuries from blunt abdominal trauma: a review. Radiol Med (Torino). 2015;120(1):21-32.
PUBMED | CROSSREF
24. Murakami R, Tajima H, Kumazaki T, Kobayashi Y. CT findings of mesenteric injury after blunt trauma. CMIG Extra Cases. 2004;28(2):11-14.
CROSSREF
25. Lee SY, Kim DW, Cho JH, Kwon HJ, Ha DH, Oh JY. CT findings of benign omental lesions following abdominal cancer surgery. J Korean Soc Radiol. 2016;75(1):1-11.
CROSSREF
26. Salama AA, Elbarbary AA, Aboryia MH. Diagnostic value of multidetector computed tomography in differentiation of benign and malignant omental lesions. Egypt J Radiol Nucl Med. 2015;46(2):305-314.
CROSSREF
27. Skipworth RJ, Fearon KC. Acute abdomen: peritonitis. Surgery. 2005;23(6):204-207.
CROSSREF
28. Broche F, Tellado JM. Defense mechanisms of the peritoneal cavity. Curr Opin Crit Care. 2001;7(2):105-116.
PUBMED | CROSSREF
29. Tirkes T, Sandrasegaran K, Patel AA, Hollar MA, Tejada JG, Tann M, et al. Peritoneal and retroperitoneal anatomy and its relevance for cross-sectional imaging. Radiographics. 2012;32(2):437-451.
PUBMED | CROSSREF
30. Kechagias A, Palomäki A, Dervenis C, Triantopoulou C. Pericolic or paracolic? The right word in the right place for acute diverticulitis. Eur Radiol. 2019;29(8):4377-4378.
PUBMED | CROSSREF
31. Bonafe T, Nicola R, Kovacs J. Differential considerations for omental fat infiltration and thickening on CT. J Am Osteopath Coll Radiol. 2014;3(4):22-24.
32. Silverman PM, Baker ME, Cooper C, Kelvin FM. CT appearance of diffuse mesenteric edema. J Comput Assist Tomogr. 1986;10(1):67-70.
PUBMED | CROSSREF
33. Seo BK, Ha HK, Kim AY, Kim TK, Kim MJ, Byun JH, et al. Segmental misty mesentery: analysis of CT features and primary causes. Radiology. 2003;226(1):86-94.
PUBMED | CROSSREF